The roticulating concept air compressor: experimental and numerical investigation

IOP Conf. Series: Materials Science and Engineering **604** (2019) 012070 doi:10.1088/1757-899X/604/1/012070

The roticulating concept air compressor: experimental and numerical investigation

Y Zhang[1], M Madamedon[1], C Copeland[1], J P Fenton[2, 5], J Subert[2], K Hinchliffe[2], I M Arbon[3] and S Leefe[4]

[1] University of Bath, Bath, BA2 7AY, UK
[2] FeTu, The Wharf, Gas Works Lane, Elland. HX5 9HH, UK
[3] Wilde Analysis, Whitworth House, 28 Charles Street, Stockport, SK1 3JR, UK
[4] Engineering Solutions Merkland Farmhouse, Pinmore, Girvan, KA26 0TE, UK
[5] Author to whom any correspondence should be addressed: info@fetu.co.uk

Abstract: This paper documents the first prototype tests of the FeTu bare-shaft oil-free air compressor, conducted over a one-year study at the University of Bath, with funding support from Innovate UK. Giving feasibility to the concept and to provide an initial indicator of its performance, in terms of pressure capability, isentropic efficiency and specific power demand as an oil-free air compressor.

A range of 6 units in total were validated on a continuous flow test-rig, with variations on internal sealing, internal clearance, and Non-Return Valve (NRV) settings, to assess their impact on volumetric efficiency, in pursuit of an optimal design.

Tests covered a speed range of 100 rpm-1500 rpm and reached discharge pressures up to 6 barg, results indicated that the compressor can maintain a 50% torque-based efficiency between a pressure ratio (PR) of 1.5 to 2.8. Tests reveal low compressed gas temperature of 125ºC at 2.8PR, which gave rise to a high isentropic efficiency of over 80%, therefore specific power was adopted as the main Key Performance Indicator (KPI).

1. Introduction

Compressed air is essential to a vast number of industrial processes and is now sometimes known as the 4th utility. It is however, a relatively inefficient form of delivering energy. The greatest energy consumption within a compressor occurs at the compression stage [1] as shown in Table 1.

Table 1*:* Summary Table of Energy Consumption [1].

Compressor Energy Consumption	**100%**
Motor Losses	10%
Compressor and idle losses	76.50%
Cooling and drying losses	1.50%
Pressure losses in filter dryer and pipework	0.50%
Leakage and expansion losses	4.50%
Compressed air	7%

70-90% of the energy used to compress air is lost in the form of heat that cannot be utilised, friction, misuse and noise [2]. The energy efficiency of compressors is becoming an increasingly important issue as many end-users seek to reduce their 'carbon footprint' by reducing energy waste and electricity consumption.

FeTu have designed a novel compression device capable of increased efficiency in the energy intensive compressor sector.

This paper analyses the first ever prototype tests of the FeTu concept at the University of Bath to demonstrate feasibility and characterise its performance in terms of pressure capability, isentropic efficiency and specific power demand in an oil-free format. The physical tests were mirrored with analytical studies to characterise the machine in a virtual environment to consider wider variables and estimate oil-injected performance.

1.1. Literature Review:

Oil-injection within State of the Art (SOA) technology, particularly within screw compressors, is common, with a fivefold purpose to act as a lubricant, reduce the temperature of compression, seal leakage, reduce sound levels and provide protection against corrosion. Despite oil injected systems having multiple filtration processes, there is still a high risk of oil contamination, therefore they can only meet class 1 ISO standards. The multiple filters do have a detrimental effect, decreasing efficiency whilst increasing installation costs, power consumption and maintenance costs [3].

Oil-free compressor technology is a growing, successful market, however certain allowances and processes must be taken for successful operation. Discussed by Almasi [4], reciprocating oil-free compressors demand special materials for rod packing, piston rings and other sealing systems that are in contact with the compressed air to avoid oil ingress; lubrication oil is still required for the crankshaft mechanism and bearings. The oil is separated from the compressed gas using a dry sealing system. The life of dry seal components is theorised to be lower compared to oil-lubricated systems due to being weaker in terms of wear and friction. Oil-free compressors are usually more expensive than oil-injected due to the specialised sealing system and expensive bearings that are needed to handle high speeds and temperatures. Additionally, it often requires a two-stage oil-free compressor [3]. Alternatively, a water-injection method in screw compressors can also be utilised as described by Dmitriev and Arbon [5]. Water-injection is predicted to provide up to 20% energy saving compared to adiabatic or dry-running compression.

Oil-free compression alone usually limits an air compressor to a pressure ratio of 3:1 due to leakage and higher discharge gas temperatures causing components to deform. If the rotors were cooled, a higher-pressure ratio could be achieved [6]. Leakage control is a prominent topic in the field of compressor research. Bell et al [7] developed a novel theoretical model based upon the isentropic nozzle able to predict the leakage flow in positive-displacement compressors. Winandy *et al* developed a simplified model, able to predict both the first and secondary parameters of a scroll compressor including electrical power, mass flow, suction heating and compression cooling levels [8].

Ooi and Shakya [9] have designed a novel rotary compressor known as the Coupled Vane Compressor where two vanes are coupled together thus creating a very compact compressor. It is predicted to offer significant savings in terms of materials used in production. Research conducted by Hu [10] focused on reducing friction within Vane compressors by introducing two roller bearings into the design. Whilst conventional vane compressors have high volumetric efficiency, mechanical friction loss is significant leading to a low coefficient of performance (COP) compared to other standard compressor types.

1.2. FeTu Concept

FeTu have created a new, novel positive displacement expander with compression capability; a compact four-chamber, single-rotor design of two symmetrical halves, bound by a single set of mechanical constraints. Two entry and two exit ports are each served by a pair of positive-displacement chambers. These dual-acting chamber pairs operate in anti-phase; in 180º rotation two chambers draw in atmospheric air through the inlet ports to the point of maximum volume, whilst their opposed partners simultaneously compress and displace air out the discharge ports to a point of zero volume.

The system; depicted in Figure 1 is made up of a single drive-shaft which runs through the device carrying a spherical rotor. The rotation of the shaft causes the rotor to 'roticulate'™ in 3D space (simultaneously rotate and articulate). The rotor follows a defined path, operating the chambers formed in the space separating the two parts. The chambers are configured in such a way that the inlet and discharge ports each receive continuous flow.

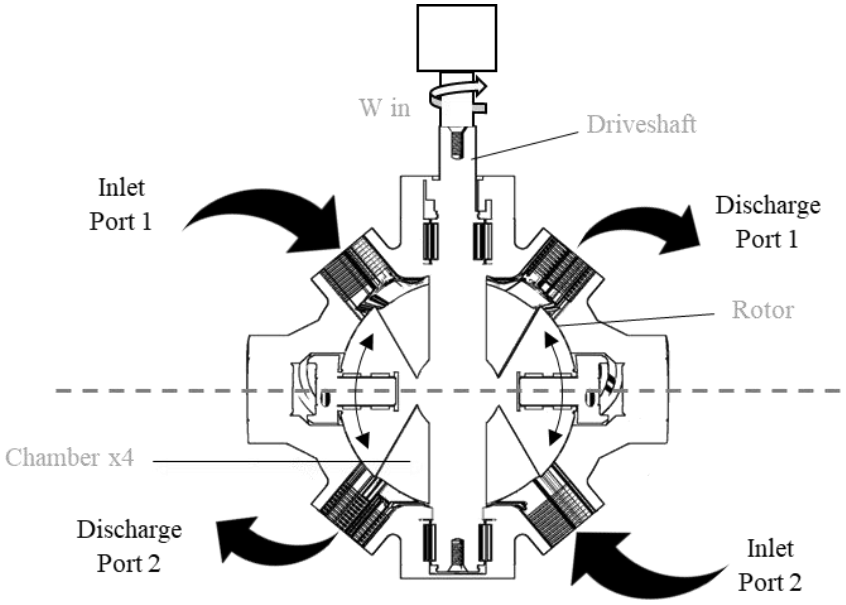

Figure 1: FeTu Concept.

The chambers rotate with the rotor, meaning they spend equal time in the compression and induction phase; this imparts a cooling effect on the internals. The proximity of the chambers as they rotate is local to the inlet during induction and local to the discharge during compression. The design makes it impossible for a chamber to be in communication with both inlet and discharge ports at the same time, meaning it can operate normally and effectively in a valveless state. The discharge port is susceptible to backflow and risks 'recompression' at high pressures in the absence of a Non-Return Valve (NRV).

The parts are made from an aircraft grade aluminium and bound within a housing of like material. The dynamic parts do not make contact but run in close proximity, sufficient to affect a seal. The leakage path lengths are long and stagnate flow through them to assist sealing. The only contact points within the device are by means of frictionless bearings. The bearings do require some lubrication; to simplify the design process, sealed-for-life units were used throughout tests. No other parts require lubrication.

Tests were done using a 120mm rotor, featuring four 0.000091m^3 chambers which each collapse to zero volume. Displacing 0.000364m^3 per revolution and completing a full cycle of each chamber in 360º, capable of delivering 0.55m^3/min free air delivery (FAD) at 1,500 rpm.

2. Test Methodology

2.1. Test rig design

A variable-speed test-rig was designed for the FeTu concept to allow pressure, temperature, torque and mass flow data to be captured as a continuous-flow process using a data acquisition and control system, recording a wide range of pressure and speed conditions. Instrumentation and valve positioning were as illustrated in Figure 2 to determine volumetric efficiency, pressure ratio, isentropic efficiency and specific power characteristics. Table 2 details each component.

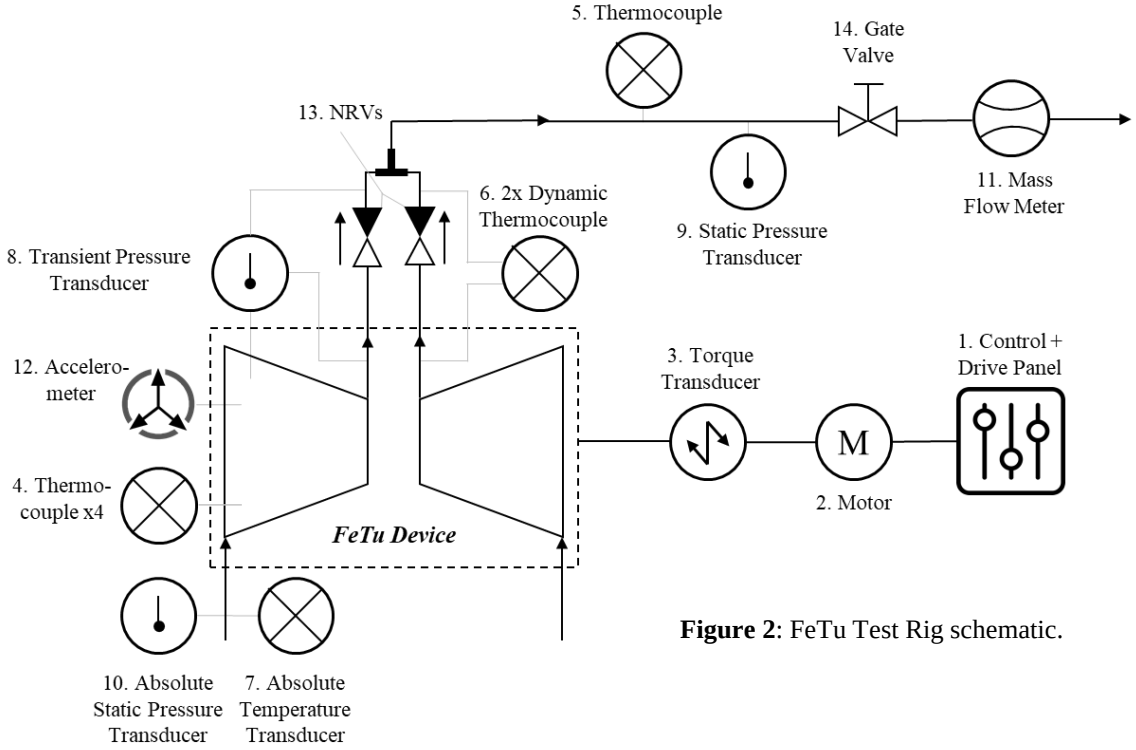

Figure 2: FeTu Test Rig schematic.

Table 2: Summary Table of Test Rig.

No.	Name	Function
1	Control Panel & DAQ	Data acquisition and control system hardware. Using SIRIUS DEWESOFT for high-frequency signals such as dynamic/transient sensors and SIERRA CP for control and average (steady state) signals such as valve opening and static sensors.
2	15kW 4 pole AC Motor	Invertor controlled variable speed motor, driving a layshaft via timing belt. Inverter set to vary torque to maintain speed setting under varying load conditions
3	KTR Torque Transducer	Inline mounted, measuring final drive input torque to the FeTu device and physical speed reference.
4	Thermocouple – on housing x3	Measuring the external steady-state temperature of the compressor body at three key positions.
5	Thermocouple - downstream	Measuring the downstream steady-state gas temperature T_{02}.
6	Dynamic Thermocouple - outlet	Measures dynamic temperature at the outlet.

No.	Name	Function
7	Absolute Temperature Transducer	Measures the atmospheric inlet temperature T_{01}.
8	Transient Pressure Transducer	Two Kistler Piezoresistive dynamic pressure sensors are installed in a position where it can partly measure the unsteady pressure in both cavities for every revolution; the other measures the unsteady pressure in the outlet port of the compressor.
9	Static Pressure Transducer	Downstream static pressure is measured p_{02}. Note: The compressor is insulated to minimize any loss of convective heat transfer.
10	Absolute Static Pressure Transducer	Measures the atmospheric inlet Pressure p_{01}.
11	V-Cone Mass Flow Meter	The V-Cone system is used to measure air velocity and density in order to calculate mass flow. Equation (8) is used to calculate volumetric flow rate from the values.
12	Accelerometer	Measures Vibration within the system.
13	NRV	Axial flow NRV (optional) were applied to the outlet ports to assess their impact on volumetric efficiency. A range of cracking pressures (pressure differential required to open NRV) were explored as detailed in Table 3.
14	Gate Valve	The manifold runs from the NRVs to the gate valve. The gate valve setting dictates the system back pressure/compressor output pressure ratio.

2.2. Test Procedure

A FeTu unit is fitted to the test rig, fully instrumented, leak-tested and lagged. Tests typically start with the gate valve fully open at 100 rpm, data is captured after system stabilisation then the pressure is increased via the gate valve, stabilised and recorded at the new pressure. A full range of pressure ratios are collected before the gate valve is fully opened once again, unit depressurised, and the speed indexed by 100 rpm. This process continues to up to 1500rpm. Therefore, there is a wide range of performance data at different pressure ratios and speeds.

Variations in clearance, NRV cracking pressure and the addition of contact seals were explored in pursuit of an optimal configuration to maximise volumetric efficiency and performance.

Table 3 below details the design variations subjected to these test conditions.

Table 3: Clearance Design choices.

Concept	Clearance (µm)	Sealing Method	NRV Cracking Pressure (PSI)	RPM Range (rpm)	Pressure Ratio (:1)
1.1	100	None	1.45	100-1100	1 - 4
1.2	50	None	1.45	100-1500	1 - 4
1.3	25	None	None, 1.45, 2.9, 4.35	100-1500	1 - 3
2.1	25	Carbon Seals	0.33	100-500	1 - 3
2.2	25	Polymer Seals	0.33	100-500	1 - 3
2.3	25	None	0.33, 1, 2.5, 5	100-1500	1 - 7

2.3. Isentropic – Temperature Based Efficiency

Firstly, the isentropic efficiency is calculated using the pressure, mass flow and temperature readings of the FeTu test rig system using Equation (1) - (4).

$$\eta_{isentropic} = \frac{P_{isentropic}}{P_{temperature}} \tag{1}$$

$$P_{isentropic} = \dot{m} c_p T_{01} \left(\frac{T_{02}}{T_{01}} - 1\right) = \dot{m} c_p T_{01} \left(\left(\frac{p_{02}}{p_{01}}\right)^{\frac{\gamma-1}{\gamma}} - 1\right) \tag{2}$$

$$P_{temperature} = \dot{m} c_p (T_{02} - T_{01}) \tag{3}$$

$$\eta_{isentropic} = \frac{P_{isentropic}}{P_{temperature}} = \frac{\dot{m} c_p T_{01} \left(\left(\frac{p_{02}}{p_{01}} \right)^{\frac{\gamma-1}{\gamma}} - 1 \right)}{\dot{m} c_p (T_{02} - T_{01})} \tag{4}$$

η, is the efficiency
P, is the Power (kW)
T_{01}, is the total gas temperature at inlet state (K)
T_{02}, is the total gas temperature at outlet state (K)
p_{01}, is the total pressure at inlet state (Pa)
p_{02}, is the total pressure at outlet state (Pa)
γ, is the specific heat ratio
$\dot{m}$, is the mass flow rate (kg/s)
c_p, is the co-efficient of pressure.

2.4. Actual Torque-Based Efficiency Calculations

The torque-based efficiency is determined by dividing the isentropic power by the calculated torque-based power. This is completed to give a second efficiency measure in Equations (5) - (7).

$$\eta_{torque} = \frac{P_{isentropic}}{P_{torque}} \tag{5}$$

$$P_{torque} = \omega * \tau \tag{6}$$

$$\eta_{torque} = \frac{P_{isentropic}}{P_{torque}} = \frac{\dot{m} c_p T_{01} \left(\left(\frac{p_{02}}{p_{01}} \right)^{\frac{\gamma-1}{\gamma}} - 1 \right)}{\omega * \tau} \tag{7}$$

ω, angular acceleration (rad/s)
τ, is the measured Torque (Nm)

2.5. Specific Power Calculations

The specific power is a value used by compressor manufacturers to assess the input power requirements in terms of the useful volumetric flowrate of the discharged air.

The volumetric flowrate of the discharge flow is determined by Equation (8), whilst Equation (9) details specific power calculation.

$$\dot{v} = \dot{m}\, \rho \tag{8}$$

$$Specific\ Power\ = \frac{P_{input}}{\dot{v}} \tag{9}$$

$\dot{v}$, is the volumetric flowrate (m^3/s)

2.6. Wilde Analysis

The FeTu design supports oil-free or oil-injected operation. During tests it was apparent, at low pressures that the design could exhibit almost 100% volumetric efficiency. Based on zero sealing losses it was felt that this could be replicated at high pressures; therefore, Wilde Analysis were recruited to conduct post-test simulation on the effects of adding oil to the Bath test data.

2.7. Vacuum Pump

Following compressor testing, the device was run oil-free in reverse against a dead head to verify its vacuum capability up to 300rpm, tests were only conducted at low speed to avoid manifold implosion. The test was repeated after introducing 40ml of oil to simulate the effects of an oil-injected system at 50 rpm.

3. Results

3.1. Sealing

Adding internal seals did not improve performance and resulted in a range of device failures.

3.2. Clearance

The internal clearance of the parts proved to have a direct correlation to the volumetric efficiency. Figures 3 and 4 plot the Volume flow-rate vs the speed for the 25µm vs 50µm design.

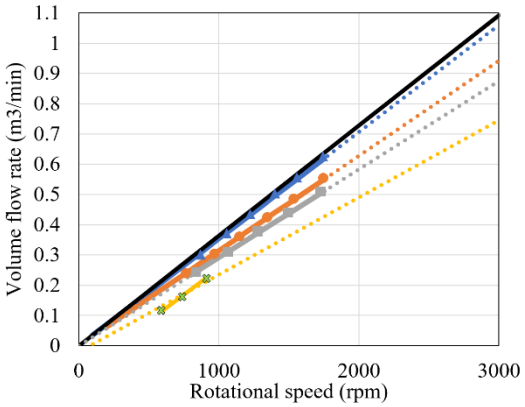

Figure 3: 25μm Vol flow rate vs speed.

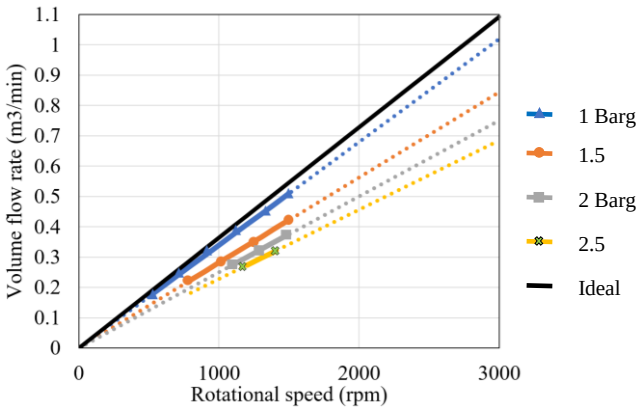

Figure 4: 50μm Vol flow rate vs speed.

3.3. NRV

At higher motor speeds (above 900rpm), the NRVs proved ineffective at preventing back flow and recompression. This is especially true in lesser spring-stiffness values, increasing the spring-rate helped but could not overcome this phenomenon. Figures 5 and 6 below show the normal NRV response at 700 rpm and an ineffective response at 1000 rpm respectively.

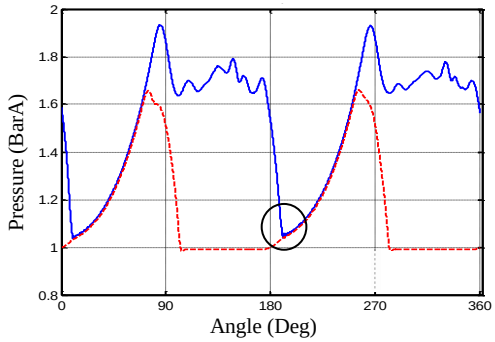

Figure 5: NRV characteristics 700 rpm.

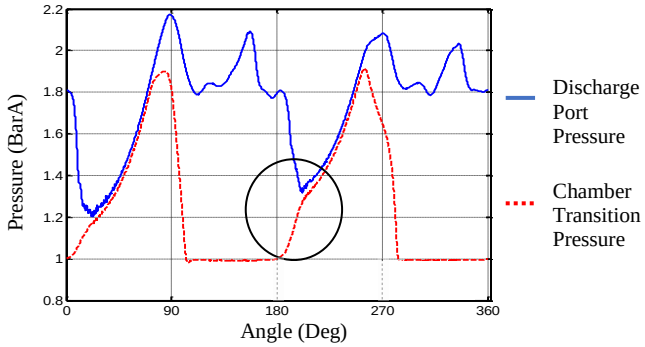

Figure 6: NRV characteristics 1000 rpm.

Figure 7 below shows that the effect of adding an NRV; typically, an NRV allows higher pressure ratios at the expense of efficiency for the same pressure ratio.

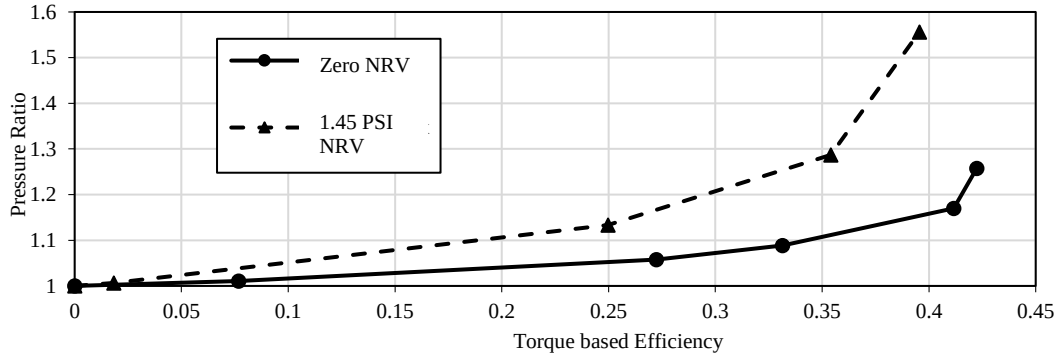

Figure 7: NRV impact.

3.4. Efficiencies

Figure 8 details the temperature-based Isentropic efficiencies calculated from Equation (4) whilst Figure 9 explains the actual Torque-based efficiency of Equation (7).

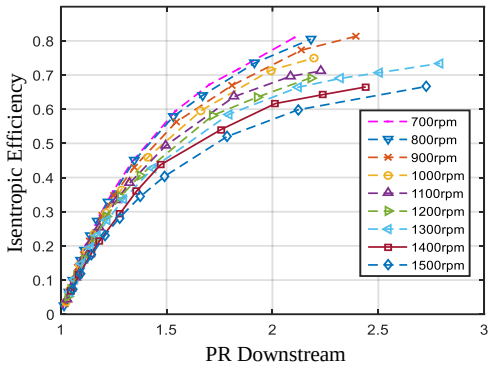

Figure 8: Temp-based isentropic efficiency.

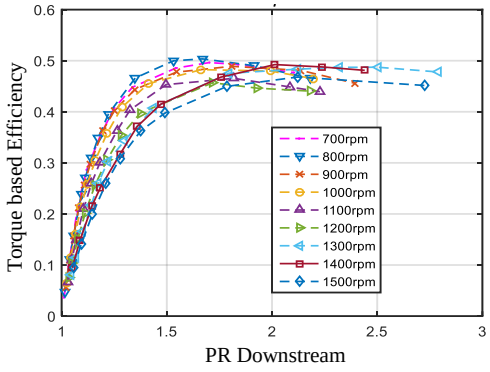

Figure 9: Actual Torque-based efficiency.

3.5. Specific Power

Figure 10 and 11 plot the volumetric flow-rate and power requirements against shaft speed respectively; each trace defines a tested pressure ratio. These are combined to produce the specific power graph as of Figure 12, calculated using Equation (9).

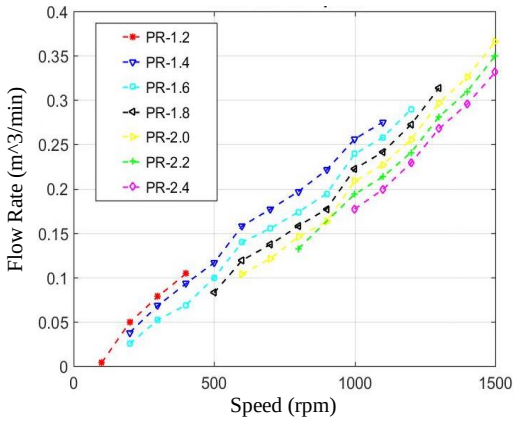

Figure 10: Flow Rate against speed.

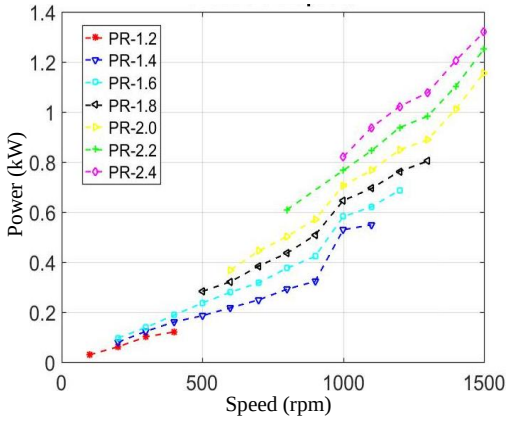

Figure 11: Power against speed.

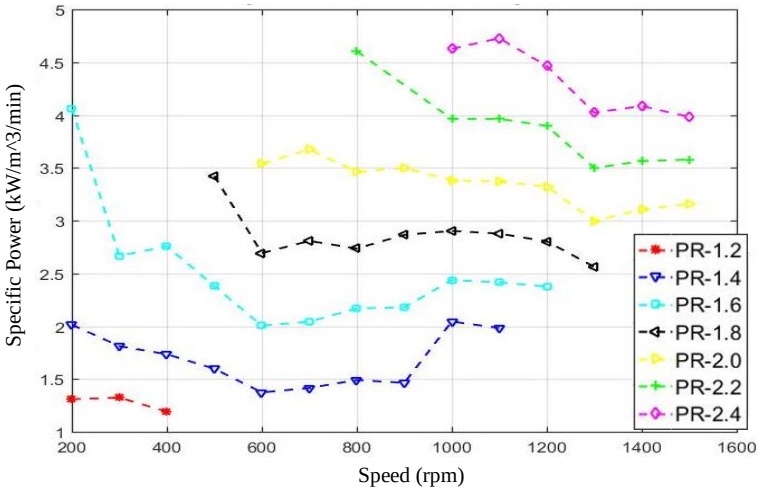

Figure 12: Specific Power against speed.

4. Discussion

4.1. Sealing

Adding physical contact seals at strategic points within the device had no effect on the volumetric efficiency but did increase torque. Performance data from unsealed versions proved most optimal. Furthermore, each sealing scheme lead to a catastrophic error within the device. The ceramic sealing fractured and entered the internal rotating parts. The polymer seal thermal expansion exceeded that of the aluminium compressor, leading to seizure.

4.2. Clearance

The 25μm clearance offered the highest volumetric efficiency as it reduced the leakage flow path throughout the device. Figures 3 and 4 shows how the volumetric flowrate is higher and closer to the ideal when using a 25μm gap. This validates 25μm as the best clearance choice from those tested.

4.3. NRV

The NRV was introduced to prevent backflow and recompression, this proved effective at reduced speeds in Figure 5. At higher motor speeds, the response time of the NRV was inadequate and back-flow was evident as depicted in Figure 6, leading to recompression and inefficiencies, evidenced by the rapid increase in chamber pressure after the 180° point.

Higher cracking pressures were introduced to overcome this phenomenon, which extended NRV effectivity to 1,200 rpm and allowed larger pressure ratios, but this did have a negative impact upon efficiency as shown in Figure 7. The NRV performance proved a limiting factor to the tests and an optimal solution is yet to be found.

4.4. Efficiencies

The initial objective of the tests was to determine the optimal isentropic efficiency; this established calculation method yielded very high values. Two factors could contribute to this phenomenon, the lag in the temperature measurement system, or the apparently low discharge gas temperature. Because of this there was a safeguard in also calculating the actual torque-based efficiency.

It was determined that the design of the device is to an extent self-cooling, due to the compression parts spending equal time in the induction and compression phase. This results in lower discharge temperatures (125ºC at 2.8 PR) which lead to an isentropic efficiency in excess of 80% as seen in Figure 8. The actual torque-based curve accounts for the internal friction within the system and reads 40-50% (above 1.5 PR) as seen in Figure 9. Over the speed ranges tested the efficiency stays relatively constant, the trending in Figures 8 and 9 validate such and show parity between calculation and instrumentation.

4.5. Specific Power

Figure 10 shows a direct correlation between rotor speed and volumetric flow and that at larger pressure ratios the volumetric efficiency reduces, leading to a reduction in flow rate. Figure 11 shows that larger pressure ratios require a higher input power within the system.

Using Equation (9) to combine these two sets of data plots, Figure 12 illustrates the specific power performance of the FeTu device. At 2.4 PR, the specific power was approximately 4-5 kW/m^3/min.

4.6. Wilde Analysis

Wilde Analysis took the Bath data and simulated the effects of adding oil. Due to the sealing effect, they predicted a significant increase in volumetric efficiently leading to pressures in excess of 7barg. Their predictions also yielded a reduction in specific power despite an increase in frictional losses in the form of oil shearing.

4.7. Vacuum Pump

The vacuum pump test was successful and demonstrated an oil-free capability to produce 0.5 bara at 300rpm. Oil was added for comparative purposes, comparing the pressure capability at just 50 rpm indicates a fivefold increase in pressure potential (50% compared to 10% vacuum). This indicates the significant effect of oil flooding on volumetric efficiency.

5. Summary

This document and the subsequent testing strategy has demonstrated the viability of the novel FeTu compressor over a wide range of operating conditions and has shown a significant potential for industry. Given this is the first test series it seems reasonable to assume the design is not yet optimal. Conclusions regarding sealing and clearance will be applied and refined in future prototypes.

Key findings:

- The compressor can develop pressure from very low speeds (100 rpm)
- Consistent Isentropic efficiency over 80% recorded. Maximum torque-based efficiency: 55%.
- The maximum pressure ratio recorded on test was 7 (6barg) at 1,000 rpm.
- Pressure capability and volumetric efficiency for a given discharge pressure, increases with speed.
- An optimal NRV setting can improve performance.
- Compressed air discharge temperatures were reassuringly low; 125ºC at 2.8 PR.

Further Work:

- Develop solutions to improve volumetric efficiency at higher pressures.
    - Run tests up to 6,000rpm (new bearing design).
    - Test the effects of oil-injection.
    - Test with fast response NRV (possibly electro-pneumatic).
- Perform long duration tests (several thousand hours) as compressor and as a vacuum pump.
- Full CFD analysis.
- To validate Wilde Analysis predictions of 7barg and low specific power against practically determined results with an oil injected compressor test rig, then compare with SOA.

6. References

[1] Doyle F and Cosgrove J 2017 An approach to optimising compressed air systems in production operations *Int. J. Ambient Energy* **39** 2 pp. 194-201

[2] Widayati E and Nuzahar E 2014 Compressed Air System Optimization: Case Study Food Industry in Indonesia *J. Phys.: Conf. Series* **105** 012018

[3] Madhav K V and Kovacevic A (2015) Economics of water injected air screw compressor systems *IOP Conf.: Mater. Sci. Eng*. **90** 012012

[4] Almasi A 2016 Latest practical notes and recent lessons learned on reciprocating compressors *Aust J Mech Eng* **14** 2 pp. 138-150

[5] Dmitriev O and Arbon I 2017 Comparison of energy-efficiency and size of portable oil-free screw and scroll compressors *IOP Conf. Ser.: Mater. Sci. Eng.* **232** 012057

[6] Stosic N, Smith I K and Kovacevic A 2012 Numerical and experimental research in heat transfer to screw compressor rotors *Front. Heat Mass Transfer* **3** 023003

[7] Bell I A, Groll E A, Braun J E, and Horton W T 2013 A computationally efficient hybrid leakage model for positive displacement compressors and expanders *Int. J. Refrig* **36** 7 pp. 1965-1973

[8] Winandy E, Saavedra C and Lebrun J 2002 Experimental analysis and simplified modelling of a hermetic scroll refrigeration compressor *Appl Therm Eng* **22** 2 pp. 107 – 120

[9] Ooi, K T and Shakya P 2018 A new compact rotary compressor: coupled vane compressor *Proc. 24th Int. Compressor Engineering Conf,* 2018 July 9-12*;* West Lafayette, USA, Purdue University Paper No. 2613

[10] Hu Y, Xu J, Wan P, Luo F and Wu F 2018 A study on novel high efficiency vane compressor. *Proc. 24th Int. Compressor Engineering Conf,* 2018 July 9-12*;* West Lafayette, USA, Purdue University Paper No. 2601.